Extension of the reactor dynamics code DYN3D to SFR applications – Part I: thermal expansion models

Nikitin, E.; Fridman, E.;

Originally published:

May 2018

Annals of Nuclear Energy 119(2018), 382-389

DOI: https://doi.org/10.1016/j.anucene.2018.05.015

Perma-Link to Publication Repository of HZDR:

https://www.hzdr.de/publications/Publ-27088

Extension of the reactor dynamics code DYN3D for SFR applications – Part I: thermal expansion models

E. Nikitin [a,b,*], E. Fridman [a], A. Pautz [b]

[a] *Helmholtz-Zentrum Dresden-Rossendorf, Bautzner Landstraße 400, 01328 Dresden, Germany*

[b] *Ecole Polytechnique Fédérale de Lausanne, CH-1015 Lausanne, Switzerland*

Keywords:

SFR, thermal expansion, nodal diffusion, Monte Carlo, Serpent, DYN3D

Abstract

The reactor dynamics code DYN3D, initially developed for LWR applications, is being extended for steady-state and transient analyses of Sodium cooled Fast Reactor (SFR) cores. In contrast to LWRs, thermal expansions of SFR core and reactor components such as fuel, cladding, diagrid, control rod (CR) drivelines, vessel, etc. provide essential reactivity feedbacks under normal and transient conditions.

Since DYN3D was originally oriented to the LWRs analyses, the modeling of thermal expansion mechanisms was not considered in the code. Therefore, the development of a new thermal-mechanical module accounting for thermal expansions has been initiated as a part of the SFR related activities. At first step, the DYN3D code was extended with the capability of treating two important thermal expansion effects occurring within the core, namely axial expansion of fuel rod and radial expansion of diagrid.

Part I of the paper provides a detailed description of the newly implemented models and presents the results of the initial verification study performed on a full core level using a large oxide SFR core from the OECD/NEA benchmark and a Phenix end-of-life core from the static neutronic IAEA benchmark.

Two IAEA benchmarks on the Phenix end-of-life experiments were used for a more detailed validation of the extended version of DYN3D. While the Part II presents the validation study performed against the static neutronic benchmark of the control rod withdrawal tests, the results of the initial stage of the natural circulation test are covered in Part III of the paper.

* Corresponding author: e.nikitin@hzdr.de

1. Introduction

The reactor dynamics code DYN3D (Rohde et al., 2016) is a best-estimate tool developed for Light Water Reactors (LWRs) applications. DYN3D comprises a 3D nodal diffusion and simplified P3 (SP3) neutron kinetics (NK) solver for rectangular and hexagonal geometries and a 1D thermal-hydraulics (TH) solver with single- and two-phase coolant flow models supplemented by fuel performance modeling capabilities.

In order to broaden its range of applicability, the DYN3D code is being adapted to steady state and transient analyses of Sodium cooled Fast Reactors (SFRs). In the framework of the SFR related methodological developments, a few-group cross section (XS) generation methodology, based on the use of the Monte Carlo (MC) code Serpent, was established (Fridman and Shwageraus, 2013a; Rachamin et al., 2013; Nikitin et al., 2015a, 2015b). The methodology was tested on different SFR core configurations demonstrating the applicability of DYN3D to steady-state analysis of SFR cores. In addition, the TH solver of DYN3D was updated to include thermal-physical properties of sodium such as thermal conductivity, density, heat capacity and viscosity.

In contrast to LWRs, SFRs are especially sensitive to thermal expansions due to the combined effect of larger temperature variations and harder neutron spectrum. In fact, thermal expansions of the core and reactor components such as fuel, cladding, diagrid, control rod (CR) drivelines, vessel, etc. provide essential reactivity feedbacks under normal and transient conditions. However, since DYN3D was originally oriented to the LWRs analyses, the modeling of thermal expansion mechanisms was not considered in the code. Therefore, the development of a new thermal-mechanical (TM) module accounting for thermal expansions has been initiated as a part of the SFR related activities. At first step, the DYN3D code was extended with the capability of treating two important thermal expansion effects occurring within the core, namely axial expansion of fuel rod and radial expansion of diagrid.

Part I of the paper provides a detailed description of the newly implemented models and presents the results of the initial verification study performed on a full core level using a large oxide SFR core from the OECD/NEA benchmark (OECD Nuclear Energy Agency, 2016) and a Phenix end-of-life (EOL) core from the static neutronic IAEA benchmark (IAEA, 2014).

The IAEA benchmarks on the Phenix EOL experiments, including control rod withdrawal tests (IAEA, 2014) and an initial stage of the natural circulation test (IAEA, 2013), were also used for a more detailed validation of DYN3D. The results of the validation study are covered in Part II and III of the paper (Nikitin et al., 2018a, 2018b).

2. Model description

2.1 DYN3D model for axial thermal expansion of fuel rods

The axial fuel rod thermal expansion reactivity effect is a combined effect of density reduction and physical elongation of the fuel rod materials. In traditional transient analyses of SFRs, TH system codes are used along with point kinetics solvers (Lázaro et al., 2014a, 2014b) where the thermal expansion effects are simply represented by the reactivity coefficients provided as input parameters. In case of spatial NK, while the density changes can be easily taken into account during the few-group XS generation procedure, additional models capable of handling changes in physical dimensions are required. In principle, it is possible to use NK solvers that are capable of solving the spatial neutronics on a deforming mesh (Fiorina et al., 2015; Patricot et al., 2016). However, the difficulty in the modeling of the axial expansion effects with existing nodal codes can be attributed to the inflexibility of the nodal mesh. Since all nodes in a same axial layer have to be of an identical height, the direct use of the fixed-mesh nodal codes restricts the modeling to a simplified case of the radially uniform axial expansion. To overcome this limitation, several approaches based on the manipulation of homogenized few-group XS have been proposed and implemented in fixed-mesh spatial NK solvers (Ponomarev and Sanchez, 2014; Reed et al., 2014; Gentili et al., 2015).

The new axial expansion model of DYN3D is designed to resolve the constraints of the fixed nodal mesh (Nikitin and Fridman, 2016). The idea of the model is to preserve the axial size of the nodes during calculations and to account for the axial expansion effects by the XS adjusting. In this way, the rigid nodal discretization can remain unchanged, and each node can be treated separately depending on its degree of expansion. The model recombines ("mixes") the XS for the affected nodes depending on the volumetric contribution of the expanded materials inside the affected node. The "mixing" model for the treatment of axial expansion implemented in DYN3D can be summarized as follows:

- Initial axial discretization is specified to account for the material boundaries at some reference temperature (e.g. as fabricated temperature) as shown in Fig. 1**Error! Reference source not found.**, left.
- The obtained axial nodes are further subdivided into a smaller node with a height of the anticipated maximal possible axial expansion of the lower node and into a bigger one as shown in Fig. 1**Error! Reference source not found.**, right.
- For each sub-assembly, local nodal temperatures are used for the estimation of the axial expansion and new material interface levels (Fig. 1, center). It should be noted that all new material levels are located within the "stripped" regions as depicted in Fig. 1**Error! Reference source not found.**, right.
- When a new material interface within the "stripped" regions is detected, the mixing of the XS is performed using flux-volume weighting:

$$\Sigma_{\text{mixed}} = \frac{h_1\Sigma_1 + h_2\Sigma_2}{h_1 + h_2} \tag{1}$$

where the indices 1 and 2 represent the lower and upper materials, *h* is the height of the material inside the "mixing" node, Σ are the original XS, and Σ_{mixed} is the final XS for the "mixing" node. The Σ includes all macroscopic reaction XS, group-to-group scattering matrices, and diffusion coefficients.

In principal, the XS mixing can be performed without specifying additional "mixing" nodes. However, axial expansion is relatively small compared to the height of the node. The XS mixing over entire "initial" nodes can lead to a so-called cusping effect (Lee et al., 1998; Dall'Osso, 2002) typical for the modeling of partially inserted control rods. This is especially problematic for the nodes with significantly different neutronic properties (e.g. adjacent fuel and sodium plenum nodes). The introduction of smaller "mixing" nodes is suggested to reduce this dilution and smearing effect.

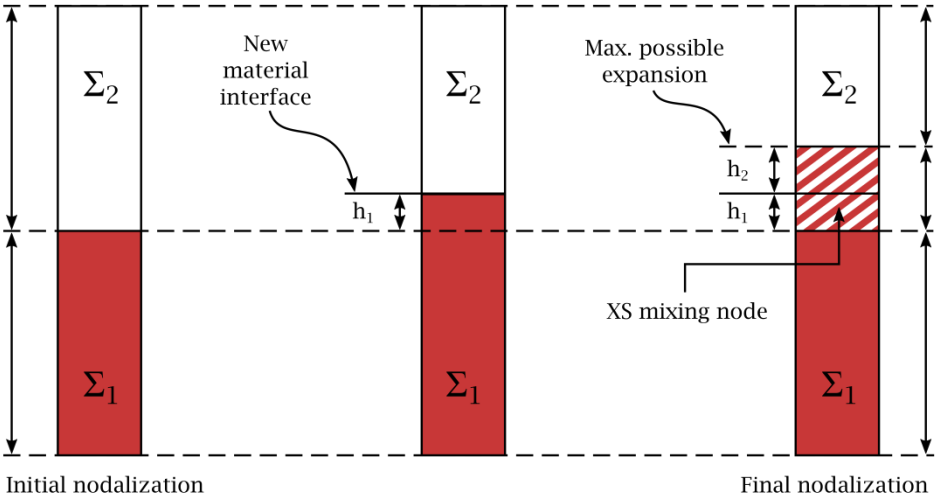

Fig. 1. Overview of the "mixing" model for the treatment of axial expansion.

The estimation of the axial expansion is performed assuming a pre-defined gas gap condition (open or closed gap). If the gap exists, then one can assume that the axial expansion of the fuel and the cladding is taking place separately. In case of a closed gap, the expanding cladding is dragging the fuel pellets upwards, i.e., the fuel and cladding expand simultaneously driven by the cladding temperature. For a more accurate modeling of the fuel-cladding interaction a coupling with a fuel performance code is needed, which is only envisaged for the later stage of the DYN3D extension.

2.2 DYN3D model for radial thermal expansion of diagrid

The diagrid located below the core acts as a sodium flow distributer and a support structure for core assemblies. The radial expansion of diagrid driven by an increase of inlet sodium temperature extends the

distance between fuel assemblies (assembly pitch) whereas the size of the assemblies (flat-to-flat distance) remains unchanged, as presented in Fig. 2. Consequently, the effective core radius is increased as well as the total sodium amount in the core. Since the former increases neutron leakage while the latter intensifies neutron captures, the diagrid expansion introduces a negative effect on reactivity.

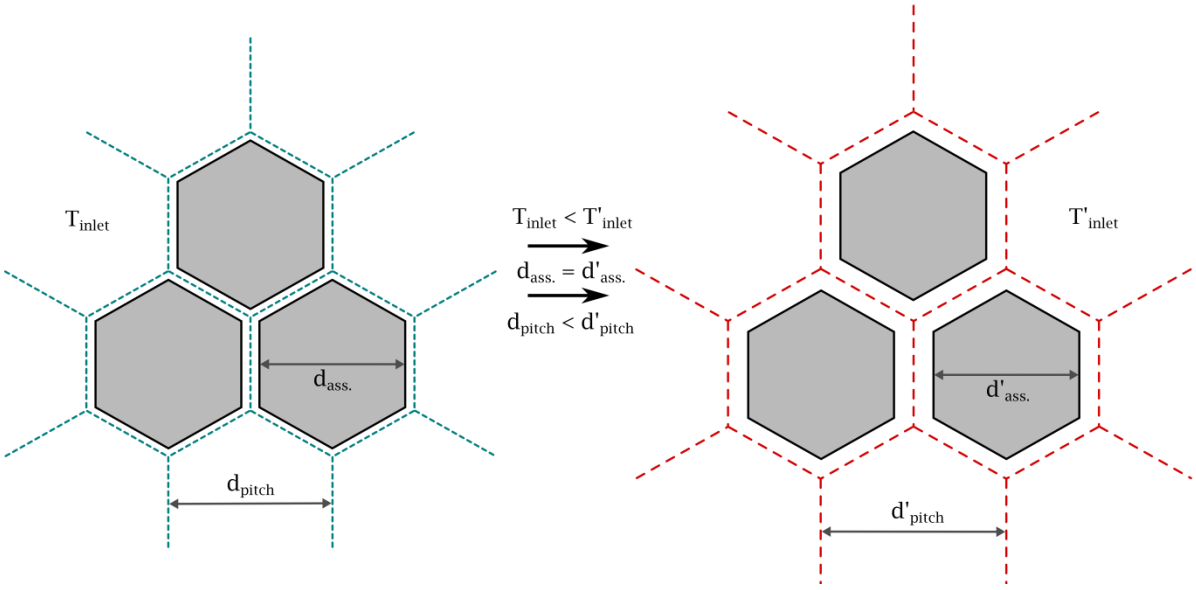

Fig. 2. Schematic overview of the radial core expansion.

The recently implemented diagrid expansion model enables the simulation of the time-dependent diagrid heat-up or cool-down, and is able to apply, respectively, the expanded or contracted assembly pitch size in the steady state and transient core calculations. The model assumes a uniform radial expansion driven by the average inlet sodium temperature. During calculations, DYN3D updates the radial hexagonal assembly pitch based on the current diagrid temperature and the corresponding linear expansion coefficient. In order to account for the thermal inertia, the time-dependent diagrid temperature is estimated using a one-dimensional cylindrical heat structure model which solves the heat equation with the Crank-Nicolson method (Crank and Nicolson, 1996). The numerical implementation of the heat structure model was verified with the approximate analytical solution of the transient heat-up of an infinitely long cylinder (Baehr and Stephan, 2006, p. 167). It should be noted that the XS data library format utilized by DYN3D was modified to introduce the assembly pitch as a new independent state parameter, which can be accounted for in the few-group XS generation process.

3. Reference cores

The performance of the newly implemented TM models was assessed in full core steady-state calculations using two reference SFR cores. The first one is a large 3600 MW_{th} mixed oxide (MOX) core (Fig. 3 left) adopted from the OECD/NEA benchmark (NEA, 2016). The second one is a small 350 MW_{th}

MOX core (Fig. 3 right) of the Phenix reactor adopted from the IAEA benchmark on the Phenix EOL experiments (IAEA, 2014).

The OECD/NEA core consists of inner and outer fuel zones loaded with 225 and 228 MOX fuel assemblies. The outer fuel zone is surrounded by 330 reflector assemblies. The core includes 24 primary and 9 secondary control rods (CR) (Fig. 3, left). The fuel assemblies comprise 271 MOX fuel pins with oxide strengthened steel (ODS) cladding. The Pu content varies between the inner and outer core zones and along the axial direction. The fuel rods are subdivided into five principal axial zones i.e. lower plenum, lower reflector, fuel, upper plenum, and upper reflector. At nominal conditions, the active core height is 100.6 cm and the assembly pitch size is 21.2 cm. Fig. 4, left presents the axial fuel rod description of the OECD/NEA core including the distribution of the Pu content.

The Phenix EOL core consists of 54 inner and 56 outer MOX fuel assemblies surrounded, first, by 86 blanket assemblies and, secondly, by 252 reflector assemblies on the periphery (see Fig. 3, right). Furthermore, the core comprises 6 primary CRs, one secondary CR, and 14 reflector-type assemblies inside the core and blanket region as depicted in Fig. 3, right. The fuel assemblies contain 217 MOX fuel pins with SS316. The fuel rods are subdivided into six axial zones including lower reflector, lower blanket, fuel, sodium plenum, upper blanket and upper reflector. The axial fuel rod layout of the Phenix core including the distribution of the Pu content presented in Fig. 4, right. At room temperature, the active core height is 85 cm and the assembly pitch size is 12.72 cm.

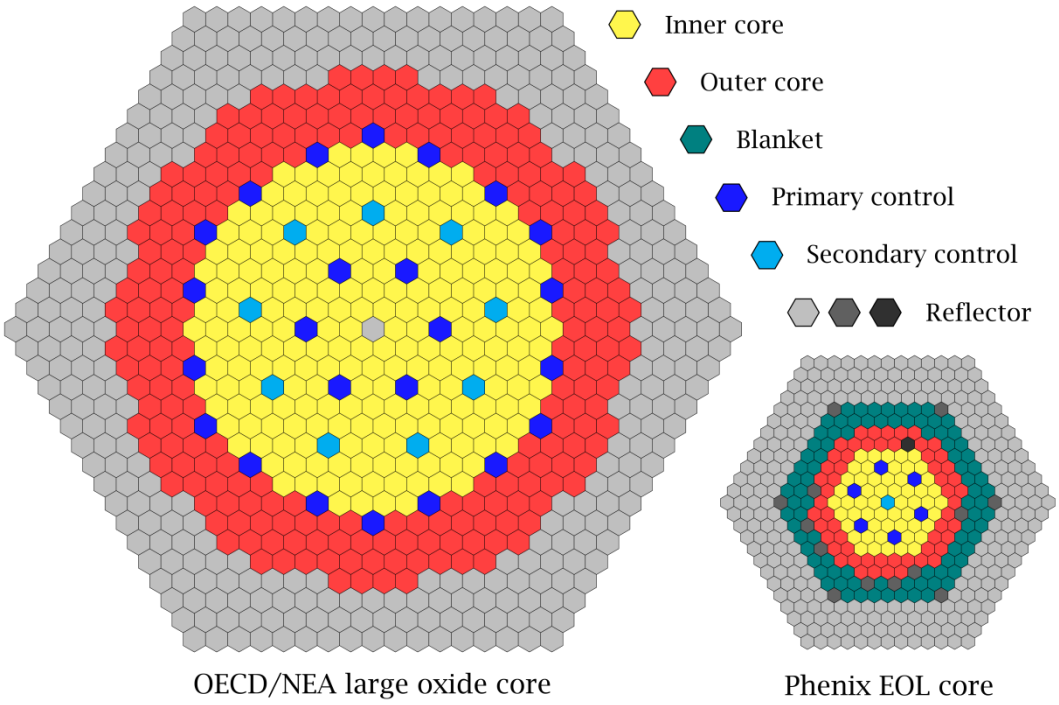

Fig. 3. References cores: radial core layout (to scale).

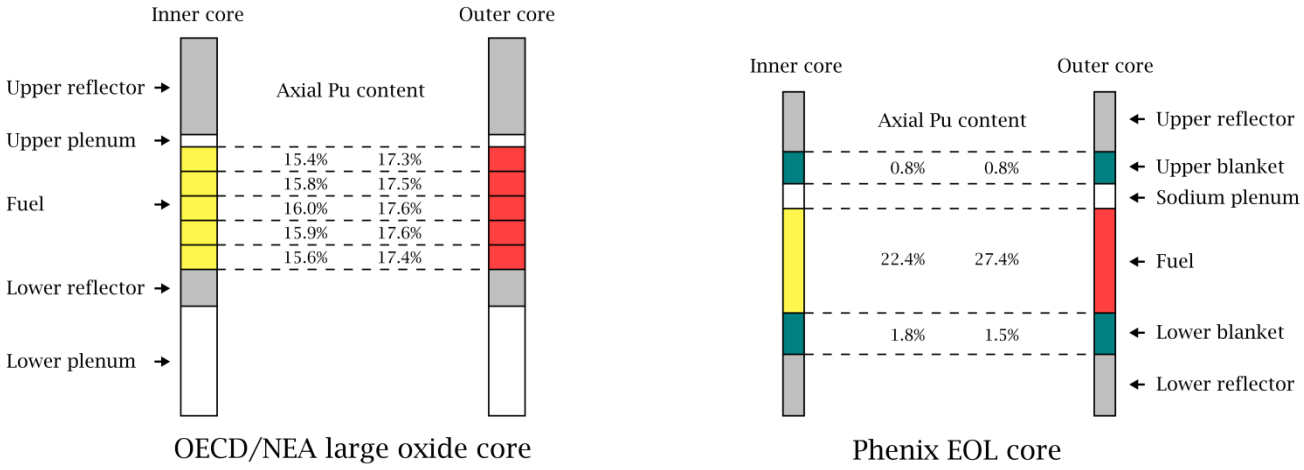

Fig. 4. Reference cores: Axial fuel rod layout (to scale).

4. Description of the test cases

The OECD/NEA and Phenix EOL cores presented in previous Section were used to test the new TM models. The references cores were expanded either axially or radially using different linear expansion coefficients. For every expansion state, a steady state DYN3D calculation has been performed while applying the new TM models. The nodal diffusion results were compared to the full core MC solutions of Serpent. In the Serpent calculations the thermal expansion was modeled explicitly, i.e. the material boundaries were physically increased and the densities of the expanded materials were reduced accordingly.

For the axial expansion modeling, it was assumed that the gas gap between the fuel pellets and cladding is closed, i.e. the expansion of fuel and cladding is driven by the cladding temperature. The fuel rods were uniformly expanded in axial direction by 0.25%, 0.45%, 0.65%, and 0.85% relatively to the reference state. The fuel and cladding densities were reduced according to the linear expansion in order to preserve the total mass. For every expansion state, the thermal expansion reactivity worth ($\Delta\rho_{exp}$) and axial power distribution were calculated by Serpent and DYN3D. The thermal expansion reactivity worth was estimated as the change in reactivity between the expanded and reference states:

$$\Delta\rho_{exp} = \rho_{exp} - \rho_{ref} \tag{2}$$

For every expansion state, the corresponding temperature was calculated using temperature dependent linear expansion coefficient and the current value of the relative thermal expansion. In this study, the linear expansion coefficients of the ODS (Hamilton et al., 2000) and SS316 (IAEA, 2014) were applied for the OECD/NEA and Phenix EOL cores respectively.

For the OECD/NEA core, the nominal state with the average core temperature of 743 K served as a reference state. Only the active core was axially expanded during the test. For the Phenix EOL core, the

isothermal state (523 K) served as a reference state. The whole fuel rods including the axial blankets and axial reflectors were expanded. In order to reduce the effect of relative CR insertion due to the upward expansion of fuel rods, the CR positions were adjusted in each expansion state to maintain the level difference between the top of the fuel rods and bottom of CRs. In both reference cores, the CRs were modeled in the complete withdrawn position, as indicated in the corresponding benchmark specification.

The radial expansion of the diagrid assumes that only the gap between the sub-assemblies is increased while the material densities, the fuel rods dimensions, the fuel pin pitch, and the dimensions of hexagonal sheath of the assemblies remain unchanged. For both reference cores, the diagrid was radially expanded by 0.3% and 1.0%. The corresponding reactivity effects were estimated by Serpent and DYN3D using Eq. 2. A larger assembly pitch size results in a higher volumetric ratio of sodium, which was also considered in regions containing homogeneous mixtures (e.g., reflectors).

5. Generation of the homogenized few-group cross sections

The few-group homogenized XS required by DYN3D were generated using the MC code Serpent. As described in Section 1, the feasibility of using Serpent for homogenization tasks was already discussed and demonstrated in the recent studies (Fridman and Shwageraus, 2013b; Rachamin et al., 2013; Nikitin et al., 2015a). Therefore, only a brief overview of the XS generation approach is provided here:

- The XS for the fuel assemblies are calculated using 3D single assembly models with reflective radial and black axial boundary conditions (BC).
- The XS for blanket sub-assemblies and all non-multiplying regions (i.e. reflectors, sodium plenums, control rods and control rod followers) are prepared using 2D super-cell models depicted in Fig. 5. All super-cells are constructed as central hexagonal region of interest surrounded by fuel assemblies. The XS are homogenized over the central hexagonal region only.
- The few-group energy structure used for the generation of the XS is a 24-group subset of the 33-group energy structure of the ERANOS code (Ruggieri et al., 2006) obtained by collapsing 10 thermal energy groups (from 24 to 33) into a single thermal group. More details regarding the selection of the few-group energy structure can be found in (Fridman and Shwageraus, 2013b; Rachamin et al., 2013).
- For further improvement of the nodal diffusion solution the Superhomogenization (SPH) technique (Kavenoky, 1978; Hebert, 1993) can be used. The SPH method was also successfully applied in nodal SFR calculations and the results were presented in (Nikitin et al., 2015b). In order to obtain the SPH factors, the MC code Serpent and nodal code DYN3D are used as the heterogeneous and homogeneous flux-solvers, respectively. In this study, the SPH factors were calculated for regions

adjacent to fuel sub-assemblies, i.e. for the sodium plenum, blanket regions, internal reflector and CR sub-assemblies.

It is worth noting that at this stage, the TH feedbacks were neglected and the fixed core average temperatures were used for all expanded states.

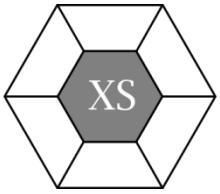

Fig. 5. 2D super-cell model for non-multiplying regions

6. Results of the test calculations

In order to test the XS mixing model, the axial expansion reactivity worth and the shift in axial power profile were calculated by the DYN3D code and compared to the MC reference. The axial expansion reactivity effects predicted by Serpent and DYN3D are presented in Table 1. It can be observed that the magnitude of the axial expansion reactivity effect in the Phenix EOL core is noticeably higher than in the OECD/NEA core due to the much smaller size of the former. For both reference core designs and all expansion states, the axial expansion reactivity worths predicted by DYN3D show a reasonably good agreement with those calculated by Serpent. The difference between diffusion and MC solutions typically stays within one standard deviation and does not exceed few pcm. It should be noted that the actual XS mixing is performed only for the expansion states of 0.25%, 0.45% and 0.65% because in case of the 0.85% expansion, the mixing nodes are completely filled with expanding material.

Table 1. Comparison of the fuel rod axial expansion reactivity worth and reactivity coefficients, Serpent vs. DYN3D.

dL/L	T, K	$\Delta\rho_{exp}$, pcm		
OECD/NEA core				
Ref.	743	Serpent	DYN3D	Difference
0.25%	924	-13 ± 3	-10	3
0.45%	1056	-27 ± 3	-29	-2
0.65%	1176	-43 ± 3	-44	-1
0.85%	1287	-60 ± 3	-57	3
Phenix EOL core				
Ref.	523	Serpent	DYN3D	Difference
0.25%	657	-48 ± 3	-51	-3
0.45%	759	-90 ± 3	-88	2
0.65%	860	-123 ± 3	-129	-6
0.85%	958	-165 ± 3	-165	0

The shift in axial power distributions due to axial expansion as calculated by Serpent is presented in Fig. 6. The radially averaged axial power profiles for all expansion states are shown in upper panels and the shift in axial power profiles are shown in lower panels. The power deviation curves clearly indicate an upward shift of the axial power profile resulting from the axial fuel rod expansion. As compared to the reference state, the sodium plenum (white background in Fig. 6) also gains power due to the introduction of the expanded fuel material into the fixed sodium plenum node. A power reduction in the lower part of the active core is more pronounced in the lowest active node of the Phenix EOL core (Fig. 6b). This can be explained by the fact, that the lower axial blanket expands into the active core, pushes out a certain amount of fuel, and, finally, reduced the power even more than in case of the OECD/NEA core (Fig. 6a).

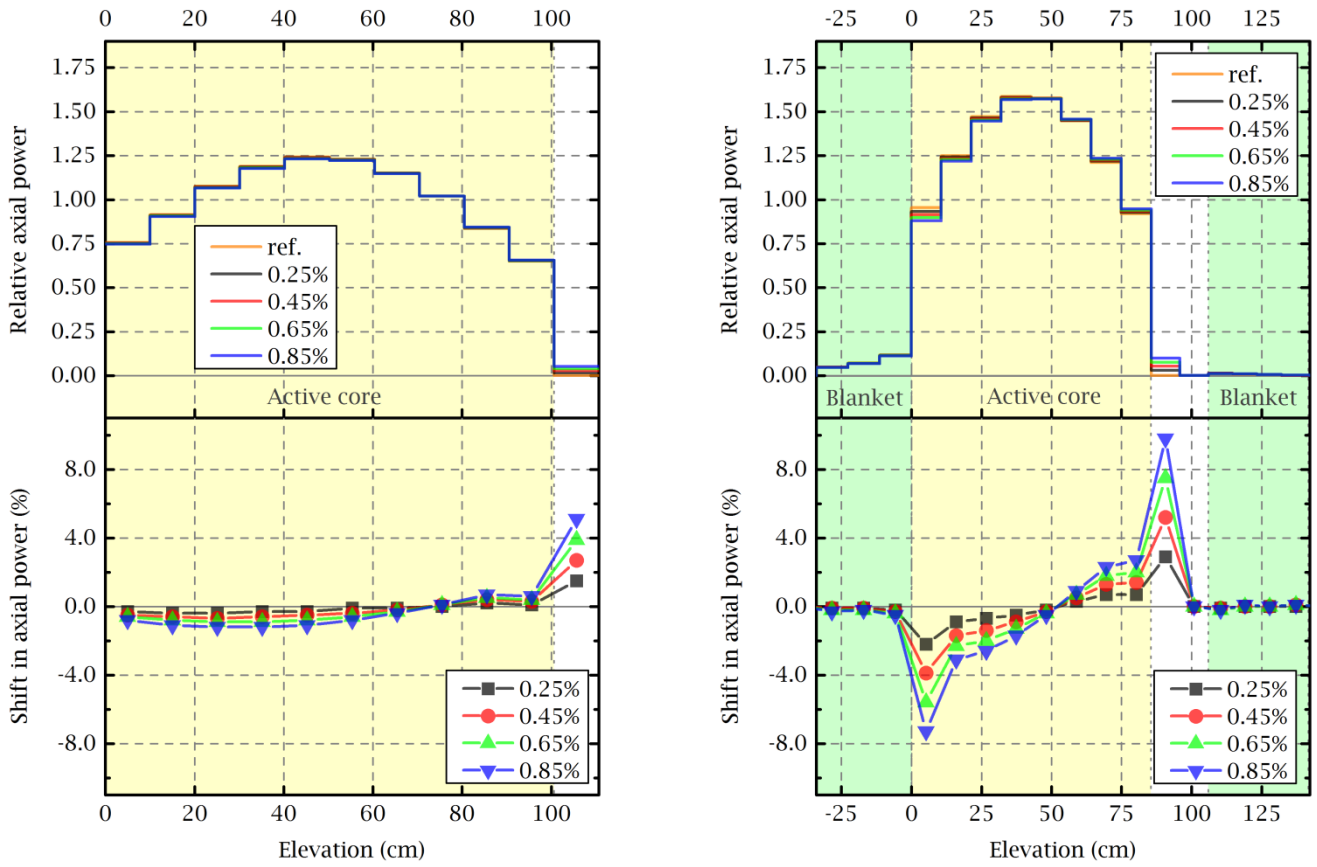

a) OECD/NEA core *b) Phenix EOL core*

Fig. 6. *Top*: Radially averaged axial power profiles for different axial expansion states; *Bottom*: shift in axial power profiles relative to the reference state. Serpent results.

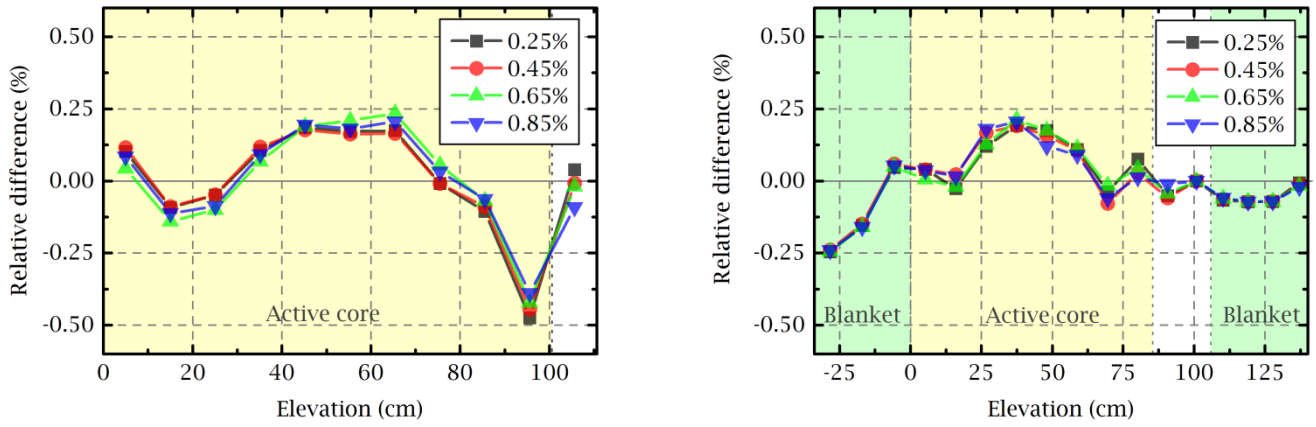

a) OECD/NEA core *b) Phenix EOL core*

Fig. 7. Relative difference in the axial power profiles for different axial expansion states, Serpent vs. DYN3D.

As demonstrated in Fig. 7, the axial power profiles predicted by DYN3D are in a very good agreement with the Serpent solutions. The maximum relative difference between Serpent and DYN3D is smaller than 1.0% and 0.3% for the OECD/NEA core (**Error! Reference source not found.**a) and Phenix EOL core (**Error! Reference source not found.**b) respectively. Fig. 7 shows a comparable magnitude of the relative error for the 0.85% expansion state, where no XS mixing due to expansion is done, and the rest of the expansion states. Therefore, it can be concluded that the smearing effect of the mixing model is relatively small.

The calculated diagrid radial expansion reactivity worths are presented in Table 2**Error! Reference source not found.**. As compared to the reference MC, the radial expansion reactivity worth calculated by DYN3D deviates up to about 20 pcm in both OECD/NEA and Phenix EOL cores. Nevertheless, the radial expansion coefficients remain in a good agreement, while roughly covering the temperature range of the liquid sodium between nominal and boiling states.

Table 2. Comparison of the radial diagrid expansion reactivity worth.

dL/L	T (K)	$\Delta\rho_{exp}$, pcm		
OECD/NEA core				
ref.	668	Serpent	DYN3D	Difference
0.30%	818	-124 ± 4	-136	-11
1.00%	1153	-429 ± 4	-428	1
Phenix EOL core				
ref.	523	Serpent	DYN3D	Difference
0.30%	683	-159 ± 4	-148	11
1.00%	1032	-529 ± 4	-507	22

7. Summary and conclusions

In SFR system analyses, the thermal expansion effects play a major role in the evolution of the transients. In order to model local expansion effects and asymmetric core behavior, 3D spatial kinetics codes with thermal expansion treatment are needed. In HZDR, the nodal diffusion code DYN3D was extended with new TM models to account for axial and radial core expansions. The axial expansion model is based on the XS "mixing" approach and capable of modeling non-uniform core expansions by using the spatial temperature distribution of the fuel rods. The radial diagrid expansion model can account for a uniform radial expansion driven by the average inlet sodium temperature.

The axial expansion model was verified for radially uniform axial expansions using the large 3600 MWth oxide core from the OECD/NEA benchmark and the smaller 350 MWth oxide core from the Phenix EOL experiments. The results were in a very good agreement with the reference MC Serpent solution showing a sufficiently good prediction of the axial expansion reactivity effect. This confirms that the implemented XS "mixing" based model is a simple and flexible way of handling the axial fuel rod expansion, which allows for an independent treatment of each fuel assembly based on local TH conditions. The concept of using expanding radial mesh in the diagrid model for the uniform radial expansion was also verified based on steady state analyses of the reference cores.

The expansion models are further assessed and validated with the help of the selected IAEA benchmarks on the Phenix EOL experiments: steady-state analysis of the CR shift test and transient calculations of an initial phase of the natural circulation test. It should be noted that the latter test is of particular importance, because in this case, the both models are applied to simulate dynamically changing axial and radial core dimensions. This is, however, a topic for Part II and III of the paper (Nikitin et al., 2018a, 2018b).

Acknowledgements

The work carried out by HZDR was partly supported by a project of the German Federal Ministry for Economic Affairs and Energy (BMWi) (registration number 150 1462).

References

Baehr, H.D., Stephan, K., 2006. Heat and Mass Transfer, 2nd ed, Physics and Astronomy. Springer-Verlag Berlin Heidelberg, Berlin, Heidelberg.

Crank, J., Nicolson, P., 1996. A practical method for numerical evaluation of solutions of partial differential equations of the heat-conduction type. Advances in Computational Mathematics 6, pp. 207–226.

Dall'Osso, A., 2002. Reducing Rod Cusping Effect in Nodal Expansion Method Calculations, in: PHYSOR 2002.

Fiorina, C., Clifford, I., Aufiero, M., Mikityuk, K., 2015. GeN-Foam: a novel OpenFOAM® based multi-

physics solver for 2D/3D transient analysis of nuclear reactors. Nuclear Engineering and Design 294, pp. 24–37.

Fridman, E., Shwageraus, E., 2013a. Modeling of SFR cores with Serpent–DYN3D codes sequence. Annals of Nuclear Energy 53, pp. 354–363.

Fridman, E., Shwageraus, E., 2013b. Modeling of SFR cores with Serpent-DYN3D codes sequence. Annals of Nuclear Energy 53, pp. 354–363.

Gentili, M., Fontaine, B., Rimpault, G., 2015. Deformed Core Reactivity Evaluation with Mesh Projection–Based Method. Nuclear Technology 192, pp. 11–24.

Hamilton, M.L., Genes, D.S., Johns, G.D., Brown, W.F., 2000. Fabrication Technological Development of the Oxide Dispersion Strengthened Alloy MA957 for Fast Reactor Applications, Pacific Northwest Laboratory.

Hebert, A., 1993. Consistent technique for the pin-by-pin homogenization of a pressurized water reactor assembly. Nuclear Science and Engineering 113, pp. 227–238.

IAEA, 2014. Benchmark Analyses on the Control Rod Withdrawal Tests Performed during the PHENIX End-of-Life Experiments, IAEA-TECDOC-1742. International Atomic Energy Agency, Vienna, Austria.

IAEA, 2013. Benchmark Analyses on the Natural Circulation Test Performed During the PHENIX End-of-Life Experiments, IAEA-TECDOC-1703. International Atomic Energy Agency, Vienna, Austria.

Kavenoky, A., 1978. The SPH Homogenization Method, in: A Specialists' Meeting on Homogenization Methods in Reactor Physics, IAEA-TECDOC-231.

Lázaro, A., Ammirabile, L., Bandini, G., Darmet, G., Massara, S., Dufour, P., Tosello, A., Gallego, E., Jimenez, G., Mikityuk, K., Schikorr, M., Bubelis, E., Ponomarev, A., Kruessmann, R., Stempniewicz, M., 2014a. Code assessment and modelling for Design Basis Accident Analysis of the European sodium fast reactor design. Part I: System description, modelling and benchmarking. Nuclear Engineering and Design 266, pp. 1–16.

Lázaro, A., Schikorr, M., Mikityuk, K., Ammirabile, L., Bandini, G., Darmet, G., Schmitt, D., Dufour, P., Tosello, A., Gallego, E., Jimenez, G., Bubelis, E., Ponomarev, A., Kruessmann, R., Struwe, D., Stempniewicz, M., 2014b. Code assessment and modelling for Design Basis Accident analysis of the European Sodium Fast Reactor design. Part II: Optimised core and representative transients analysis. Nuclear Engineering and Design 277, pp. 265–276.

Lee, K.B., Joo, H.G., Cho, B., Zee, S., 1998. Correction of the Control Rod Cusping Effect Using One-Dimensional Fine Mesh Flux Profiles, in: Korean Nuclear Society Autumn Meeting.

NEA, 2016. Benchmark for Neutronic Analysis of Sodium-cooled Fast Reactor Cores with Various Fuel Types and Core Sizes, NEA/NSC/R(2015)9. OECD Nuclear Energy Agency. https://www.oecd-nea.org/science/docs/2015/nsc-r2015-9.pdf

Nikitin, E., Fridman, E., 2016. Axial fuel rod expansion model in nodal code DYN3D for SFR application, in: PHYSOR 2016.

Nikitin, E., Fridman, E., Mikityuk, K., 2015a. Solution of the OECD/NEA neutronic SFR benchmark with Serpent-DYN3D and Serpent-PARCS code systems. Annals of Nuclear Energy 75, pp. 492–497.

Nikitin, E., Fridman, E., Mikityuk, K., 2015b. On the use of the SPH method in nodal diffusion analyses of SFR cores. Annals of Nuclear Energy 85, pp. 544–551.

Nikitin, E., Fridman, E., Pautz, A., 2018a. Extension of the reactor dynamics code DYN3D for SFR applications – Part II: validation against the Phenix EOL control rod shift tests. Annals of Nuclear Energy, submitted.

Nikitin, E., Fridman, E., Pautz, A., 2018b. Extension of the reactor dynamics code DYN3D for SFR applications – Part III: validation against the initial phase of the Phenix EOL natural convection test.

Annals of Nuclear Energy, submitted.

OECD Nuclear Energy Agency, 2016. Benchmark for Neutronic Analysis of Sodium-cooled Fast Reactor Cores with Various Fuel Types and Core Sizes, NEA/NSC/R(2015)9. OECD Nuclear Energy Agency.

Patricot, C., Baudron, A.-M., Fandeur, O., Broc, D., 2016. Neutronic calculation of deformed cores: Development of a time-dependent diffusion solver in CAST3M, a mechanics dedicated finite element code, in: PHYSOR 2016.

Ponomarev, A., Sanchez, V., 2014. Modeling of reactivity effects and non-uniform axial expansion of SFR core on basis of neutronics model with constant calculation mesh, in: International Congress on Advances in Nuclear Power Plants, ICAPP 2014.

Rachamin, R., Wemple, C., Fridman, E., 2013. Neutronic analysis of SFR core with HELIOS-2, Serpent, and DYN3D codes. Annals of Nuclear Energy 55, pp. 194–204.

Reed, M., Smith, K., Forget, B., 2014. The "Virtual Density" Theory of Neutronics: A Generic Method For Geometry Distortion Reactivity Coefficients, in: PHYSOR 2014.

Rohde, U., Kliem, S., Grundmann, U., Baier, S., Bilodid, Y., Duerigen, S., Fridman, E., Gommlich, A., Grahn, A., Holt, L., Kozmenkov, Y., Mittag, S., 2016. The reactor dynamics code DYN3D – models, validation and applications. Progress in Nuclear Energy 89, pp. 170–190.

Ruggieri, J.M., Tommasi, J., Lebrat, J.F., Suteau, C., Plisson-Rieunier, D., De Saint Jean, C., Rimpault, G., Sublet, J.C., 2006. ERANOS 2.1: International code system for GEN IV fast reactor analysis, in: Proceedings of the 2006 International Congress on Advances in Nuclear Power Plants, ICAPP'06.